Published in Journal of Hydrology 332, issues 1-2, 158-173, 2007
which should be used for any reference to this work

The role of tributary mixing in chemical variations at a karst spring, Milandre, Switzerland

J. Perrin [a,*], P.-Y. Jeannin [b], F. Cornaton [a]

Summary Solute concentration variations during flood events were investigated in a karst aquifer of the Swiss Jura. Observations were made at the spring, and at the three main subterraneous tributaries feeding the spring. A simple transient flow and transport numerical model was able to reproduce chemographs and hydrographs observed at the spring, as a result of a mixing of the concentration and discharge of the respective tributaries. Sensitivity analysis carried out with the model showed that it is possible to produce chemical variations at the spring even if all tributaries have constant (but different for each of them) solute concentrations. This process is called tributary mixing. The good match between observed and modelled curves indicate that, in the phreatic zone, tributary mixing is probably an important process that shapes spring chemographs. Chemical reactions and other mixing components (e.g. from low permeability volumes) have a limited influence.

Dissolution-related (calcium, bicarbonate, specific conductance) and pollution-related parameters (nitrate, chloride, potassium) displayed slightly different behaviours: during moderate flood events, the former showed limited variations compared to the latter. During large flood events, both presented chemographs with significant changes. No significant event water participates in moderate flood events and tributary mixing will be the major process shaping chemographs. Variations are greater for parameters with higher spatial variability (e.g. pollution-related). Whereas for large flood events, the contribution of event water becomes significant and influences the chemographs of all the parameters. As a result, spring water vulnerability to an accidental pollution is low during moderate flood events and under base flow conditions. It strongly increases during large flood events, because event water contributes to the spring discharge.

KEYWORDS Karst hydrology; Groundwater chemistry; Spring chemograph; Solute transport; Mixing; Numerical model

[a] *Centre of Hydrogeology, Neuchâtel University, 11 rue E-Argand, 2007 Neuchâtel, Switzerland*
[b] *Swiss Institute of Speleology and Karstology, case postale 818, 2300 La Chaux-de-Fonds, Switzerland*

[*] Corresponding author. Present address: Department of Earth Sciences, 200 University Avenue, University of Waterloo, Waterloo, Canada N2L 3G1. Tel.: +1 519 888 4567x5261; fax: +1 519 883 0220.
E-mail address: jperrin@uwaterloo.ca (J. Perrin).

Introduction

Water chemistry of karst springs can show significant variations during a hydrological year. These variations are generally related to flood events (Kiraly and Mueller, 1979; White, 1988; Dreiss, 1989; Vervier, 1990), and to annual cycles for some parameters. The observed changes during flood events are considered to be linked to the organised heterogeneity of karst aquifers, which can be described as a network of high permeability conduits embedded in low permeability limestone volumes (Kiraly, 1998). The conduit network usually shows a dendritical pattern (Palmer, 1991), somewhat similar to surface drainage networks. However, karst conduit networks can be three dimensional. The upper part of the karstic network, where infiltration takes place, is named epikarst or subcutaneous zone (Mangin, 1975; Williams, 1983). This zone is responsible for the allotment of recharge water between the underlying conduits and the low permeability volumes (also known as matrix storage). This complexity of the karstic network is responsible for a duality in recharge conditions (concentrated in the conduits, diffuse in the low permeability volumes), in storage capacity (high in the low permeability volumes, low in the conduits), and in flow velocities (high in conduits, low in the low permeability volumes).

Time concentration curves at karst springs are often called chemographs. During flood events, chemograph variations at karst springs are generally explained by the mixing of different types of waters. Models of spring chemographs usually consider the following end-members contributing to a flood event: concentrated recharge, diffuse recharge and water stored in the low permeability volumes (Vervier, 1990), phreatic water and fresh infiltrated water (Kiraly and Mueller, 1979; Blavoux and Mudry, 1983), epikarst storage, conduit storage, and fresh infiltrated water (Williams, 1983; Sauter, 1992; Lakey and Krothe, 1996), mixing of several tributaries (Hess and White, 1988), rapid delayed recharge water and water stored in the low permeability volumes (Plagnes and Bakalowicz, 2001). Birk et al. (2006) described in detail the interactions between conduits and low permeability volumes with the help of numerical simulations.

In some studies (Shuster and White, 1971; Ternan, 1972; Groves, 1992; Wicks and Engeln, 1997; Grasso and Jeannin, 2002; Grasso et al., 2003), decrease of dissolution-related parameters during flood events is explained by calcite dissolution kinetics: the flood waters flow too quickly as compared to base flow, and do not reach the thermodynamic equilibrium with respect to calcite, providing a decrease in ion concentration along the flood. Similar reactive models, depending on process kinetics, are being applied for the simulation of heat transport in karst systems. Heat exchange between the flowing water and the rock matrix is therefore considered instead of chemical reactions (Benderitter et al., 1993; Birk et al., 2001, 2002, 2004). Birk et al. (2005, 2006) assessed the potential effect of water stored in the low permeability volumes on chemographs and tracer breakthrough curves.

All these models are based on observations of karst springs. Detailed investigations inside a karst aquifer (Milandre test site) have been carried out for about 10 years to assess the adequacy of existing models to describe the relevant physical processes occurring within a karst system. A conceptual diagram of the aquifer (Fig. 1) shows that three main tributaries feed the karstic spring. Hydrographs and chemographs from both the upstream part of the phreatic zone (i.e. where the tributaries reach the master conduit) and the spring were studied. This information is used to assess the role of the (trivial) mixing of tributaries, which in the following will be referred to as ''tributary mixing'', on spring chemographs and hydrographs. Field observations are therefore interpreted by considering tributary mixing only, along the flow path of an underground river, which is recharged by three main tributaries. To do so, a one-dimensional flow and transport model including tributary mixing is used to reproduce the hydrographs and chemographs observed during flood events. If the tributary mixing model fits the observed data, it can be assumed that matrix storage, dissolution kinetics or any other kind of mixing may have a limited influence on the chemographs shape.

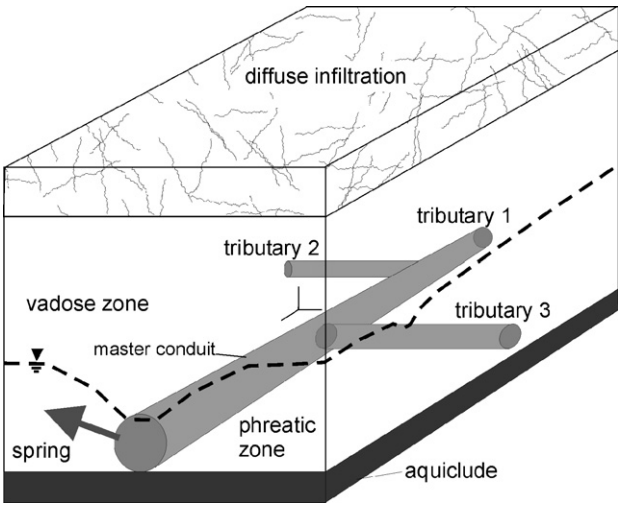

Figure 1 Conceptual diagram of the studied aquifer. The conduit network is schematically represented by grey tubes. The phreatic zone is constituted by the master conduit and the surrounding low permeability volumes which also correspond to the matrix storage.

Study area and methods

The Milandre test site is part of a karstic aquifer located in the Swiss tabular Jura in the vicinity of Basle (Fig. 2). The outlets of the system are the Saivu spring, which has a discharge rate ranging between 20 l/s and 200 l/s, and the Bame temporary spring, which can show discharge rates higher than 1500 l/s. A small part of the total discharge by-passes the springs and directly feeds an alluvial aquifer further downstream. On the basis of numerous tracer-test experiments and a water budget (Gretillat, 1996; Jeannin, 1998), the catchment area is estimated to be around 13 km^2. The land-use is constituted by pasture, forestry, arable land, and local settlement. The soil thickness varies from absent to a few metres, and mainly consists of highly cohesive silty loam. Thicker soils are generally colluvial.

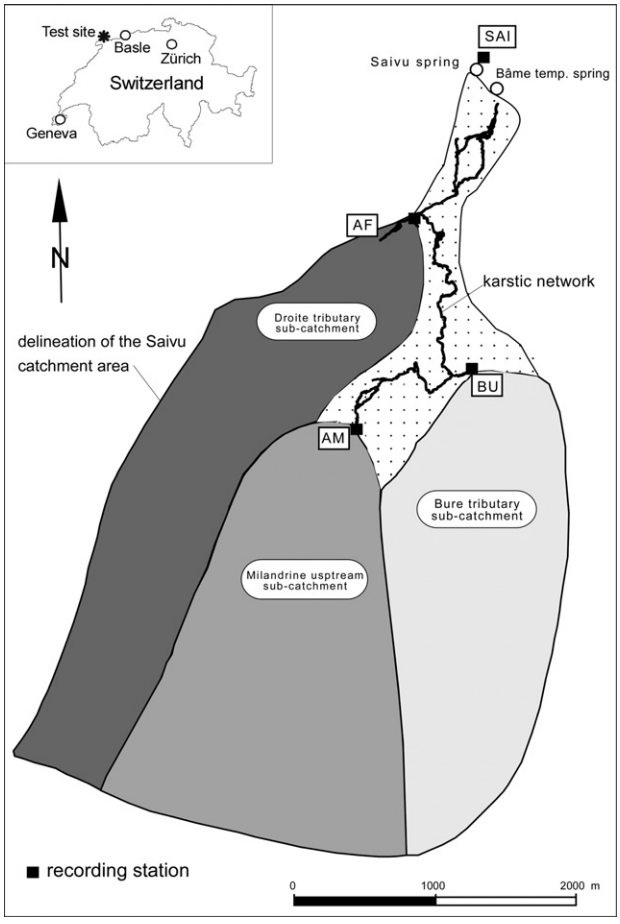

Figure 2 The catchment area of the Milandre karst aquifer is a plateau recharged by diffuse infiltration. It is divided in four sub-areas: The sub-catchment areas of Droite (AF), Milandrine upstream (AM), and Bure (BU) tributaries are indicated in grey. Their respective surface area ranges between 3.6 and 4.5 km^2. The part of the basin that is drained by small tributaries connected to the underground river is represented by the dotted surface. The karstic network (total length of 10.5 km) is only accessible in the downstream part of the system (modified after Grasso and Jeannin, 1994).

Annual precipitations in the area are close to 1000 mm, half of which recharging the karst aquifer by diffuse recharge mainly. A well developed karstic network, located 50—80 m below ground surface, drains the aquifer towards the Saivu and Bame springs (Fig. 2). Water levels measured in piezometers located in the low permeability volumes, close to the major conduits, are systematically higher than the levels measured in the cave (Jeannin, 1998), evidencing groundwater storage in the neighbouring fissured matrix. However, discharge measurements along the cave during dry hydraulic conditions showed that the contribution from the fissured matrix is lower than 10% of the underground river discharge (Maréchal, 1994).

The Saivu spring (SAI) originates from the Milandrine underground river. Speleologists can explore the underground conduit over a distance of 4600 m. In the cave, three main tributaries are encountered: about 35% of the total discharge comes from the Milandrine upstream tributary (AM), 30% from the Bure tributary (BU), and 30% from the Droite tributary (AF). The remaining discharge (5%) is issued from secondary tributaries and low permeability volumes. Perrin et al. (2003a) showed a strong relation between land use and ground water chemistry of the respective tributaries: the AM and BU catchments show evidences of human activities, whereas the AF catchment is still well preserved (Table 1).

Water levels were continuously recorded at AM, BU, the Saivu spring (SAI), and the Bame temporary spring and discharge rates were then determined from a rating curve. Unfortunately, discharge cannot be derived from water levels at AF because the conduit is completely flooded during high water events. Specific conductance was continuously recorded at AM, BU, AF, and SAI. These data were calibrated using regular manual measurements. Nitrate concentrations were continuously recorded at AM following the procedure presented by Perrin and Wenger (2001).

As far as chemical investigations were concerned, groundwater was sampled at AM and SAI (results will be presented below). For each sample, specific conductance and temperature were measured on site, pH was determined within 12 h at sampling temperature, bicarbonate within 24 h by titration, and the other parameters were analysed

Table 1 Main physico-chemical characteristics (average and coefficient of variation) of the spring and main tributaries of the Milandre karst system

	Flow [l/s]	Cond [μS/cm]	K^+ [mg/l]	Cl^- [mg/l]	NO_3^- [mg/l]	HCO_3^- [mg/l]
Average						
AM	69.55	610.4	2.38	12.00	24.22	351.9
BU	44.16	586.9	2.30	8.71	17.08	344.1
AF	39.10	571.2	0.44	7.42	16.14	340.8
SAI	140.25	598.7	1.94	10.50	21.55	349.0
CV [%]						
AM	79.08	5.77	46.48	19.47	17.45	5.09
BU	75.00	5.72	24.07	14.79	17.36	7.52
AF	86.45	2.46	14.38	15.38	22.98	2.97
SAI	65.07	3.94	51.90	22.87	19.19	6.73

These data are based on 12 monthly sampling campaigns. (Adapted from Perrin et al., 2003a.)

by ionic chromatography after a 0.45 μm filtration. For cation preservation, filtered samples were acidified to pH <2 with HNO_3 suprapur. Nitrate concentrations in samples containing methanal or not were equivalent; therefore no methanal was added in the samples. The data quality was checked using ionic balances. Raw data are available at the following web address: http://capella.unine.ch/chyn/usr/perrin/jerome.html. Nitrate and bicarbonate concentrations are respectively given in mg NO_3^-/l and mg HCO_3^-/l throughout the paper.

The chemical parameters presented in the study have been selected for their contrasting chemographs. Three parameters are derived from external sources (fertilisers mainly): nitrate, chloride and potassium. The spatial distribution of these parameters is heterogeneous, yielding contrasting chemographs. They are called ''pollution-related parameters''. The other parameters (bicarbonate, calcium, specific conductance) are representative of the limestone dissolution process. They are called ''dissolution-related parameters''. Their spatial distribution is more homogeneous (Perrin et al., 2003a).

Observed nitrate chemographs for two flood events of increasing importance have been selected and are shown in the next section. The chemographs are simulated with the tributary mixing model (see Section 'Numerical modelling'). The same model is then applied to specific conductance chemographs recorded during one flood event at all observation points. Finally a comparison between nitrate and specific conductance chemographs is given. Note that the data presented in this paper are part of a larger study and that more complete observations are available in Perrin (2003).

Field data

October 2000 flood event

Hydrographs and chemographs description

Following a 3 weeks dry period, a flood occurred in the morning of October 11th. The flood began after continuous rainfall had started. Daily recharge calculated by the model of Jeannin and Grasso (1995) is 2.8 mm for that day. Discharge at Milandrine upstream (AM) increased at 8 a.m., and Saivu spring (SAI) about 2 h later. This flood event was relatively small with a maximum discharge in the Bame–Saivu system of less than 420 l/s (Fig. 3). The response to recharge is rapid (a few hours) and the pulse duration is limited (one day).

Chemographs were separated in four successive phases (Fig. 3): At AM, (1) pre-event water flowed until the 11th at 11:00–11:30 a.m., i.e. during a large part of the rising limb of the hydrograph. (2) Peak flood water was characterised by lower concentrations in bicarbonates and nitrates and a progressive increase in chloride and potassium. (3) Falling limb water showed an increase for all ions. (4) Recession water was characterised by a slight decrease in bicarbonate. Nitrates still increased but chloride and potassium stabilised.

At Saivu spring, (1) pre-event water showed stable parameters until the 11th at 2 p.m., when the Bame temporary spring reached its flood maximum. (2) Peak flood water was characterised by a slight concentration decrease for nitrates and potassium. (3) On the falling limb, chloride and potassium showed an increase in concentration, while nitrates continued to decrease. (4) Recession water was characterised by an increase in nitrates and a stabilisation of other parameters at values slightly higher than pre-event water. Bicarbonate remained fairly stable throughout the flood event, except for a short positive peak at the beginning of the event.

Qualitative interpretation

Significant concentration changes appear clearly in pollution-related parameters. A decrease in NO_3^- started at 11:15 a.m. at AM, and 2 h 45 min later at SAI, that is about 4 h later than the arrival of the flood pulse. The increase in Cl^-, K^+ started at 1:40 p.m. at AM, and 3 h 20 min later at SAI. Finally the NO_3^- increase started at 3:15 p.m. at AM, and at 6 a.m. the following day at SAI.

These variations can be interpreted as a consequence of tributary mixing: the first 4 h correspond to the piston phase of flow during which the water stored in the conduit between the more downstream tributary (AF) and the spring is flushed. The flushed volume can be derived from the hydrograph, by calculating the integral of discharge throughout the piston phase duration. The calculated volume is 4000 m^3 and the distance between AF tributary and the spring is 1400 m. Thus, the flooded conduit cross-section, which is simply the flushed water volume over the conduit length, is about 2.8 m^2. This area is in good agreement with the direct observations in the cave. Initial variations at the spring cannot be produced by AM waters since the travel time ranges between 6 h for very high discharge rates and 15 h for low water conditions (Maréchal, 1994). It is very probable that nitrate dilution at the spring originates from the preferential contribution of AF tributary, which has low nitrate concentration (Perrin et al., 2003a). The increase in chloride and potassium can be linked to the preferential contribution of BU tributary, which is more polluted than AF. AM is the tributary which is the most heavily contaminated with nitrate. The increase in nitrate at the spring corresponds to that observed at AM with a time lag of 14 h 45 min, giving a flow velocity of 330 m/h. This velocity falls in the range of the measured velocities in the Milandre underground stream (Maréchal, 1994; Jeannin and Maréchal, 1995).

January 2001 flood event

Hydrographs and chemographs description

This flood started January 24, 1 h 30 min after the first input of rain, and lasted until the 29th. The event can be separated into three successive floods of decreasing magnitude (A, B, and C in Fig. 4), each one being linked to a rainfall event: calculated daily recharge is 17 mm the 24th, 7 mm the 25th and 7.5 mm the 27th. Prior to the flood, hydraulic conditions had been stable for about two weeks.

Only flood A was sampled in details. Chemographs were separated into three successive phases (1, 2, 3 in Fig. 4): At AM, pre-event water (1) lasted until 3:30 p.m. on the 24th, 2 h 30 min after the discharge started to increase. Peak flood water (2) showed concentrations that decreased

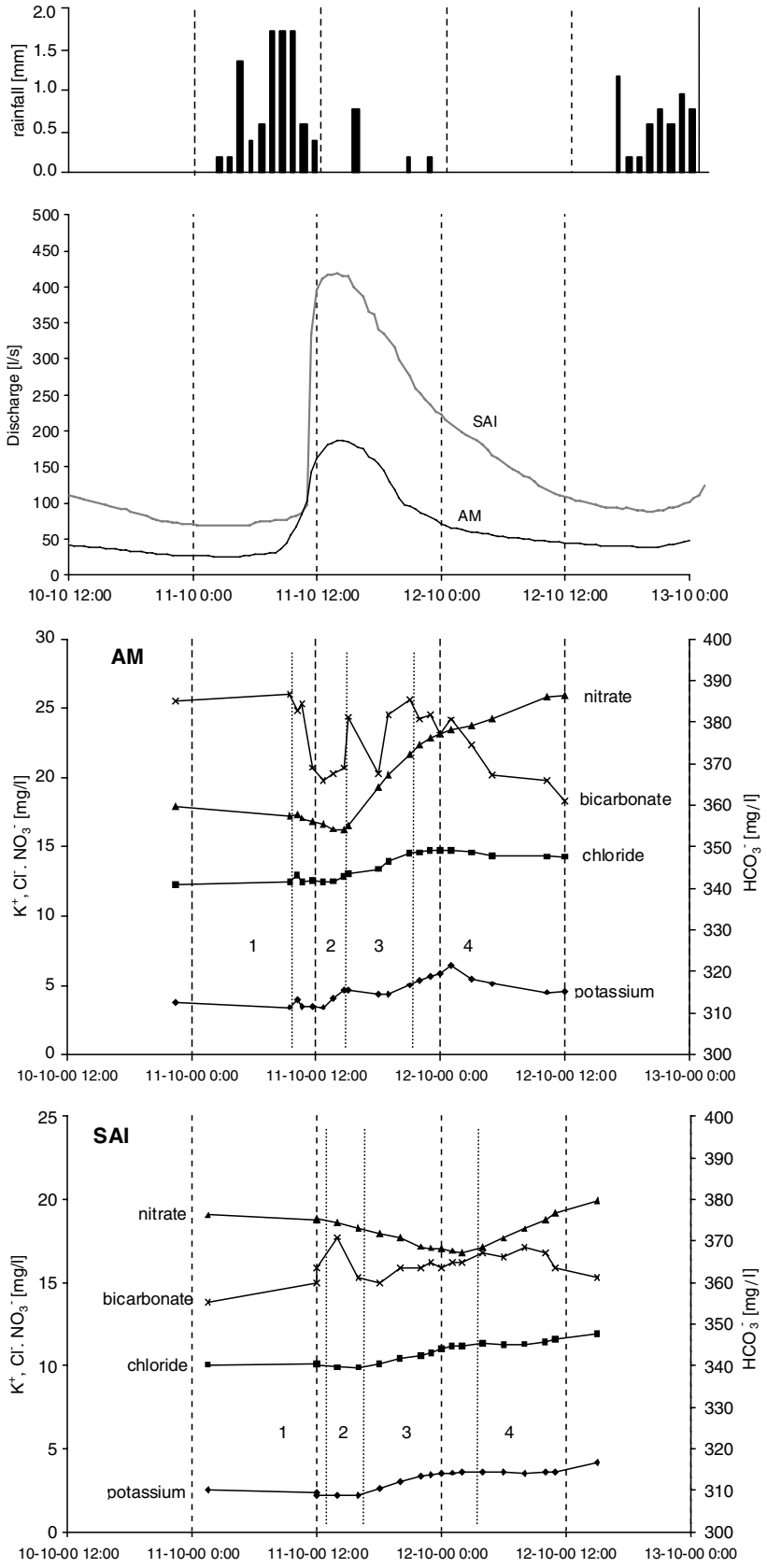

Figure 3 October 2000 flood event: discharge measurements at AM and SAI (upper graph) and rainfall; chemographs at AM and SAI (lower graphs).

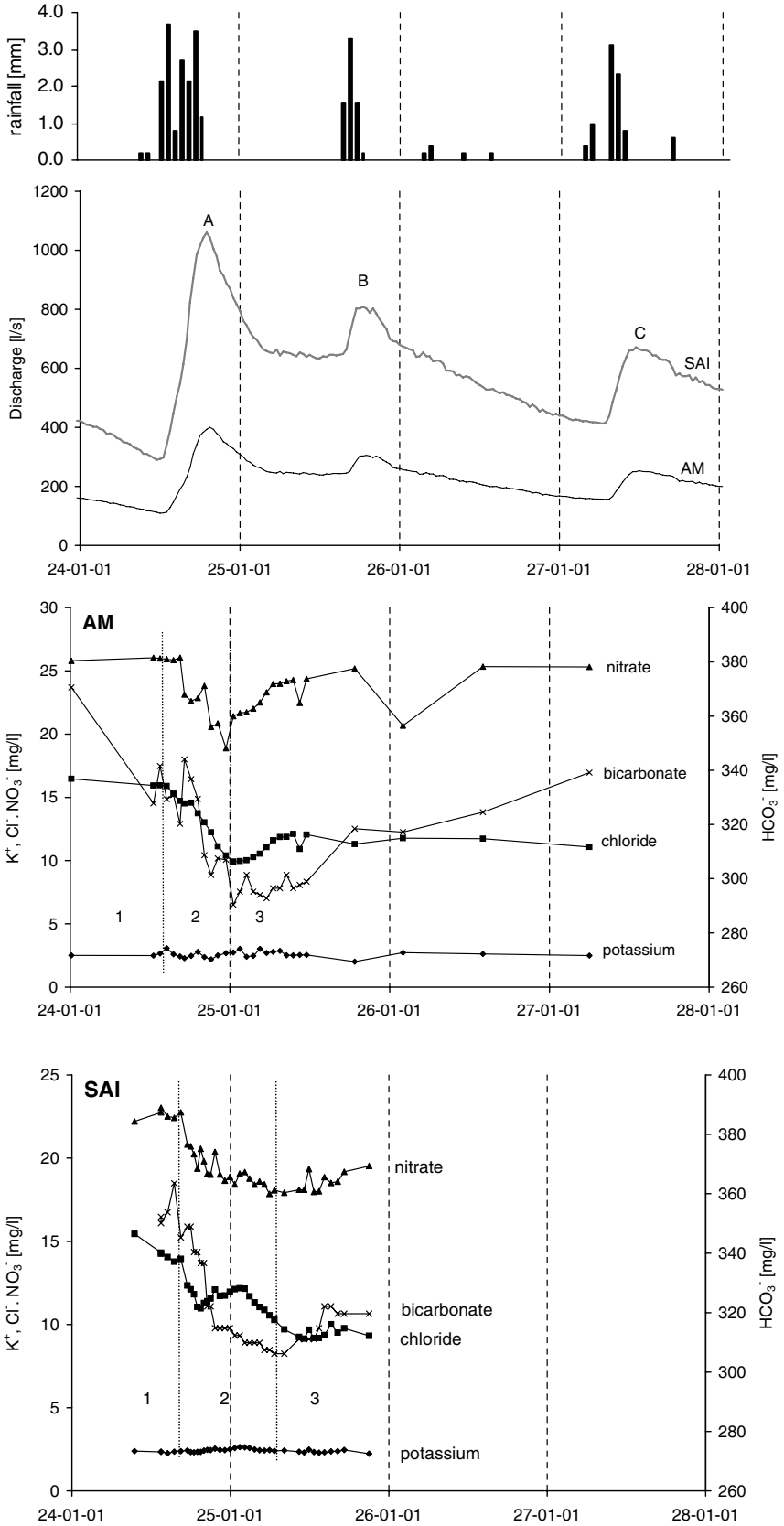

Figure 4 January 2001 flood event: discharge measurements at AM and SAI (upper graph) and rainfall; chemographs at AM and SAI (lower graphs).

for bicarbonate and chloride from 3:00 p.m. onwards. Nitrate started to decrease 2 h 30 min later. Falling limb water (3) was characterised by a concentration increase in chloride, bicarbonate and nitrate starting early the 25th. The recovery was quite complete for nitrate and bicarbonate by the 27th. In contrast, chloride remained at lower concentrations.

At the Saivu spring, pre-event water (1) flowed during 4 h after the discharge increase. Peak flood water (2) was characterised by a decrease in nitrate, bicarbonate, and chloride. For chloride, a secondary peak was visible. Falling limb water (3) showed concentrations that recovered progressively with time. Potassium at SAI and AM did not show any clear change during the event.

Qualitative interpretation

The overall trend is described by a decrease in chlorides, nitrates and bicarbonates concentration of nearly 20% during the peak discharge. The major difference between AM and SAI is the existence of a peak in chloride at SAI during the flood climax. Like for the October 2000 flood event, the spring chemographs can be explained by tributary mixing. The piston phase lasted 4 h, which corresponds to a volume of 5000 m^3. This volume is higher than that of the previous flood event, as a consequence of a more important pre-event discharge. Therefore the flow cross-section in the conduit is larger. Preferential contribution by the AF tributary induces a general dilution. During the flood peak, the influence of more contaminated tributaries (BU and AM) results in a chloride peak, followed by a dilution corresponding to the arrival of AM diluted waters. For all ions excepting bicarbonate, minimum concentrations at AM and SAI are the same (within 1 mg/l). For bicarbonate, the minimum concentration increased from 290 mg/l at AM to 305 mg/l at the spring. This change may indicate possible dissolution along the horizontal flow path towards the spring.

Conclusions

We observed that the chemographs at AM and SAI have several differences: concentrations are systematically lower at SAI when compared to AM; nitrate and chloride variations are modified at SAI compared to those observed at AM. The hypothesis, which is tested in the following section, is that the contributions of the BU and AF tributaries, located downstream of AM, determine the SAI chemographs through mixing. Such a mixing has already been identified under steady-state flow conditions (Perrin et al., 2003a). Hence, under transient flow conditions tributary mixing in the phreatic zone is supposed to influence the shape of SAI spring chemographs. This hypothesis is further assessed by applying a 1D numerical model of groundwater flow and transport. This type of model implicitly includes tributary mixing.

Numerical modelling

A conceptual model was designed and solved numerically in order to simulate hydraulic and chemical responses at the Saivu spring in a very simple way. The model takes into account the following three tributaries: Milandrine upstream (AM), Bure (BU), and Droite (AF), which are hydraulically connected by a 1 D conduit. Their combination is supposed to reproduce the spring response (SAI). Although this model is a strong simplification of the reality, its main objective is to test the effect of tributary mixing on a qualitative basis.

Characteristics of the numerical model

Simulations were carried out using a transient flow and transport one-continuum finite element simulator developed at the Centre of Hydrogeology of the University of Neuchâtel (Cornaton, 2004). The model provides a pre-solution of the velocity field for each time-step by solving the 1D flow equation under confined conditions. Advective-dispersive transport is then solved by making use of the pre-computed velocity field. The developed model of the Milandre system is 1D since it focuses on the pipe network only. The pipe section integrated 1D flow equation can be formalized by the following equation:

$$\pi r_c^2 S_c \frac{\partial H}{\partial t} + \tilde{\nabla} \times \left(\pi r_c^2 K_c \tilde{\nabla} H\right) = \pm \pi r_c^2 Q \tag{1}$$

where t is time, r_c [L] is the pipe radius, K_c [LT^{-1}] and S_c [L^{-1}] are the pipe hydraulic conductivity and specific storage coefficient respectively, $H = H(x, t)$ [L] the hydraulic head, and Q a source/sink intensity [T^{-1}]. The hydraulic conductivity K_c [LT^{-1}] is obtained from the Hagen–Poiseuille formula,

$$K_c = \frac{\rho g}{\mu} \frac{r_c^2}{8}, \tag{2}$$

where ρ denotes the fluid density [ML^{-3}], g the acceleration of gravity [LT^{-2}] and μ the dynamic viscosity [$ML^{-1}T^{-1}$]. The specific storage coefficient S_c is obtained by neglecting the skull deformation (Cornaton and Perrochet, 2002)

$$S_c = \frac{\rho g \theta}{E_w} \tag{3}$$

where θ is the mobile water content [–] and E_w the compressibility of water [$ML^{-1}T^{-2}$]. The pipe network conductive and capacitive parameters are deduced from (2) and (3) by integrating over the pipe section, $K = \pi r_c^2 K_c$ [$L3T^{-1}$] and $S = \pi r_c^2 S_c$[L]. The pipe section integrated 1D transport equation can formalized by:

$$\pi r^2 \frac{\partial \theta C}{\partial t} = -\tilde{\nabla} \times \left(\pi r^2 (qC - D\tilde{\nabla} C)\right) \tag{4}$$

where $C = C(x, t)$ is the resident concentration [ML^{-3}], and where q [LT^{-1}] and D [$L^2\ T^{-1}$] are the fluid flux and dispersion coefficient respectively:

$$\begin{aligned} q &= -K_c \nabla H \\ D &= \alpha_L q + \theta D_m \end{aligned} \tag{5}$$

In Eq. (5), α_L denotes the coefficient of longitudinal dispersivity [L] and D_m the coefficient of molecular diffusion [L^2T^{-1}]. Eqs. (1) and (4) are solved by using a standard Galerkin finite element formulation, and the time-derivatives are handled by a finite difference approximation, according to the classical non-diffusive Crank–Nicholson scheme.

The geometry of the model is based on the Milandre conduit network (Fig. 5). A main conduit of 4766 m length is

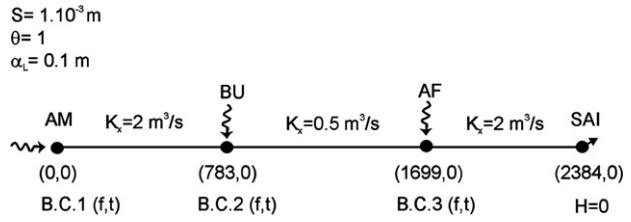

Figure 5 Main characteristics of the 1D numerical model. The boundary conditions are indicated by a dot with the corresponding coordinates. B.C. (f,t) means boundary conditions for flow and transport.

meshed with 2383 two-noded pipe elements (2384 nodes). The length of each finite element is 2 m.

The flow and transport boundary conditions can be formalized as follows: A nodal source is prescribed at each inlet node (nodes corresponding to the inlet AM, and to the tributaries BU and AF in Fig. 5), $Q = Q_0(t)$, and a constant hydraulic head $H = 0$ m is used to model the outlet (Saivu spring SAI). For transport, imposed concentrations $C = C_0(t)$ are used at inlet AM and at the tributaries BU and AF.

The model was used by running simulations in order to fit the observed spring hydrographs and chemographs. Hydraulic heads are not considered since they do not have a real meaning in the system. In fact, an important limitation of the model is that it is based on Darcian flow in pipes, for which the relationship between flow velocity and discharge is linear. In real karst systems, this is rarely the case. Therefore, the values of the parameters K and S also have a poor physical meaning for the modelled system. They must be regarded as confined porous medium equivalent parameters (cf. Hagen—Poiseuille law for K), which allow for an acceptable representation of the velocity field distribution within the pipe network in such a way that advective-dispersive transport can still be realistic.

Calibration of flow and transport parameters

Several simulations were carried out in order to test the sensitivity of the model response to various sets of hydraulic and transport parameters. The most realistic hydrographs and chemographs shapes were obtained by using the following values: Pipe section integrated hydraulic conductivity (K) between 0.5 and 10 m^3/s and storage coefficient (S) of 0.001 m, a porosity (θ) of 100%, and a longitudinal dispersivity (α_L) of 0.1 m. These values are consistent with previous studies: Cornaton and Perrochet (2002) used a hydraulic conductivity of 10 m^3/s and a storage coefficient of 0.005 m for an analytical modelling of karst spring hydrographs. Jeannin (2001) also used an effective hydraulic conductivity ranging between 1 and 35 m^3/s for modelling head and flow distribution in the Hölloch cave system. Note that the adopted value for the storage coefficient does follow the straight application of Eq. (3), which considers water compressibility only, yielding very small values for S. Since confined flow conditions are used in the model, we need to increase artificially the value of S in order to obtain a realistic diffusive property (K/S). A confined model cannot account for karst specific storage processes during a rainfall event, like e.g. the rising of free water levels in open conduits. The cave (real system) is oversimplified in the applied model: the underground stream, which is an open channel flow with turbulent flow conditions, is simulated by a straight confined laminar pipe. However Hauns et al., 2001) showed that after a certain distance (typically 200—300 m) mixing and dispersion processes lead to very similar results in a confined pipe or in an open flow channel. In this case, tracer breakthrough curves through a turbulent open channel can be well described by a laminar confined conduit. The modelled system has the adequate length for using the laminar flow in confined conduits approach. Moreover the aim of this simple model is to test the role of tributary mixing only without accounting for other potential transport processes such as complex flow along the channel.

The hydraulic conductivities were defined in order to reproduce the observed flow velocities at medium water stage (50 l/s at AM). In the cave, measurements of flow velocity showed variations between the upstream part of the conduit and the spring. Based on tracer tests, Jeannin and Maréchal (1995) found the following velocities for a discharge rate of 50 l/s at AM: 500 m/h between AM and BU, 300 m/h between BU and AF, and 500 m/h from AF to the spring. In the numerical model K was fixed at 0.5 m^3/s for the slower velocity section and 2 m^3/s for the two other sections (Fig. 5) in order to fit to the observed flow velocity. Zero initial hydraulic heads were set at all nodes, and the model was run for 80 h with constant flow and imposed concentration at the three tributaries in order to reach steady-state conditions for flow and transport prior to the flood event simulation. All the simulations were carried out with the same set of flow and transport parameters (Fig. 5). The only changes between simulations were the boundary conditions at AM, BU, and AF (B.C. 1, 2, 3).

Model sensitivity to boundary conditions

For the simulations presented in Section 'Modelling of the Observed Chemographs', some boundary conditions had to be inferred (no field measurements available): AF flow boundary conditions, AF and BU nitrate chemographs. Therefore the sensitivity of the model to uncertainties in flow and transport boundary conditions has been tested. It showed that: (1) Simulated chemographs at SAI spring (output of the model) are not very sensitive to inflow boundary conditions (i.e. discharges assigned to each tributary), showing that strong variations of the water flux input are necessary to produce significant changes in the chemographs. Increasing discharge at AF by a factor 4 leads to a maximum change in spring concentrations of 7%, and a maximum offset between peaks of 1 h. This is especially true because the chemographs at AM, BU, and AF are in the same concentration range. (2) Chemographs at SAI are quite sensitive to modifications on transport boundary conditions. If a constant concentration instead of a time-dependent chemograph is used at one of the tributaries, peaks on the spring chemographs will disappear.

In summary, uncertainties in tributary discharge measurements will have a limited effect on simulated spring chemographs, whereas uncertainties in tributary chemographs will have more impact on simulated spring chemographs.

Theoretical case

A simple case was first simulated in order to point out the role of tributary mixing (Fig. 6). Flow boundary conditions are identical for the three tributaries in the first simulation and are identical for BU and AF but slightly different for AM in the second simulation. Transport boundary conditions are kept constant, but different for the three tributaries. The concentrations are fixed at 22 mg/l for AM, 15 mg/l for BU, 10 mg/l for AF.

The modelled spring chemograph presents clear variations with pre-event stable concentration (mixing of three tributaries with stable discharge rate), followed by a decrease during the rising limb (more water comes from AF at this point), and a concentration increase during the falling limb (more water coming from AM). Thus, due to mixing, the model produces temporal variations in concentration at the spring although input concentrations are kept constant at the three tributaries. If such variations would be observed with real data, it could theoretically be possible to predict the existence of tributaries with different chemical signatures. Moreover, their relative distance to the spring could be inferred. In our example, the early concentration decrease indicates a tributary with low concentrations close to the spring (AF), and the late concentration rise indicates a tributary with high concentrations further upstream (AM). If flow velocity is known (e.g. from tracing experiments), time to peak concentrations (negative or positive) may be used to infer the distance from the tributary to the spring. Different input discharge curves (illustrated by the second simulation) lead to slight changes in the spring chemograph such as an accentuated negative peak; however the general chemograph shape is maintained.

Modelling of the observed chemographs

In the following section, the nitrate chemographs of the two analysed flood events were modelled. Nitrate was chosen because very contrasting responses can be observed at the spring, as well as contrasting concentrations in the three tributaries (Perrin et al., 2003a), and because it has a conservative behaviour in the conduit network.

Flow rates at AF were not continuously measured, nor were the chemographs at BU and AF. Hence, flow and transport boundary conditions at the three tributaries were fixed as follows: Measured nitrate concentration and discharge rate at AM, measured discharge rate and fixed concentration (based on monthly analyses) at BU, equivalent discharge to BU and fixed concentration (based on monthly analyses) at AF. Discharge at AF is known to differ little from that of BU based on 10 discharge measurements. The selected concentrations for BU and AF correspond to the mean annual values calculated from 14 samples: 17 mg/l at BU, and 16 mg/l at AF. For the October 2000 flood event, the fit was improved by using the slightly different concentrations of 21 mg/l at BU, and 20 mg/l at AF.

October 2000 flood event

The simulated discharge rate is in agreement with the observed hydrograph (Fig. 7). The flood peak is sharper, but this difference can be due to uncertainties in storage coefficient S and/or in the observed data (existence of losses in the phreatic zone). The simulated chemograph reproduces a slight decrease in concentration, but 7 h later than the observed one. If this decrease is due to AM tributary, then flow velocity is underestimated by the model. However, it is also possible that a decrease in concentration occurred in the other tributaries (data not available).

The total discharge rate at SAI spring can be subdivided into three hydrographs corresponding to the volume of water issued from each tributary (Fig. 7). The relative contribution of the tributaries throughout the flood is clearly illustrated: AF water predominates during the rising limb because this tributary is the closest to the spring, BU water dominates during the falling limb, and the end of the flood is mainly constituted by AM water. The secondary peak of AM

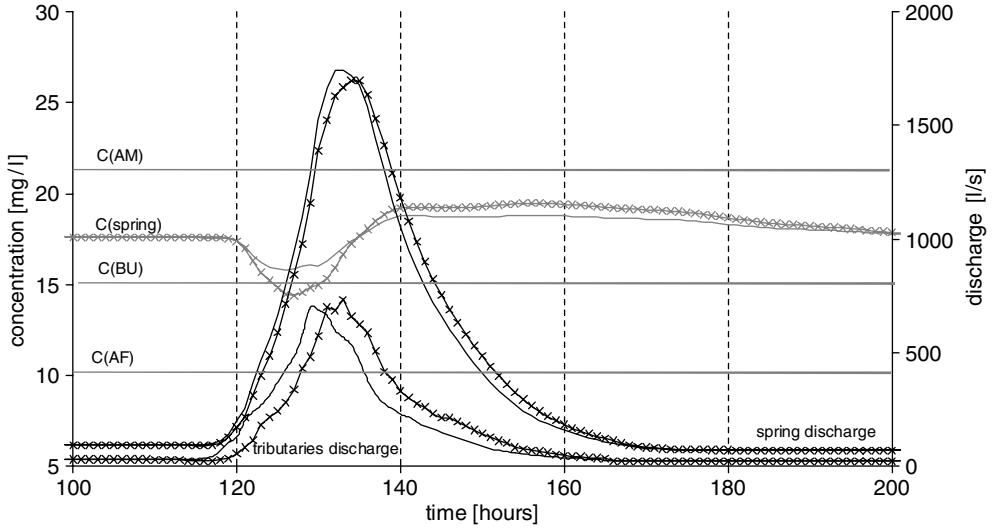

Figure 6 Numerical simulation of theoretical boundary conditions (grey lines for concentrations, black lines for discharge). Two results corresponding to different flow boundary conditions are presented: the first is obtained with identical tributary discharge (represented by the plain curve), the second lines with symbols is obtained with identical discharge for BU and AF and a different discharge for AM.

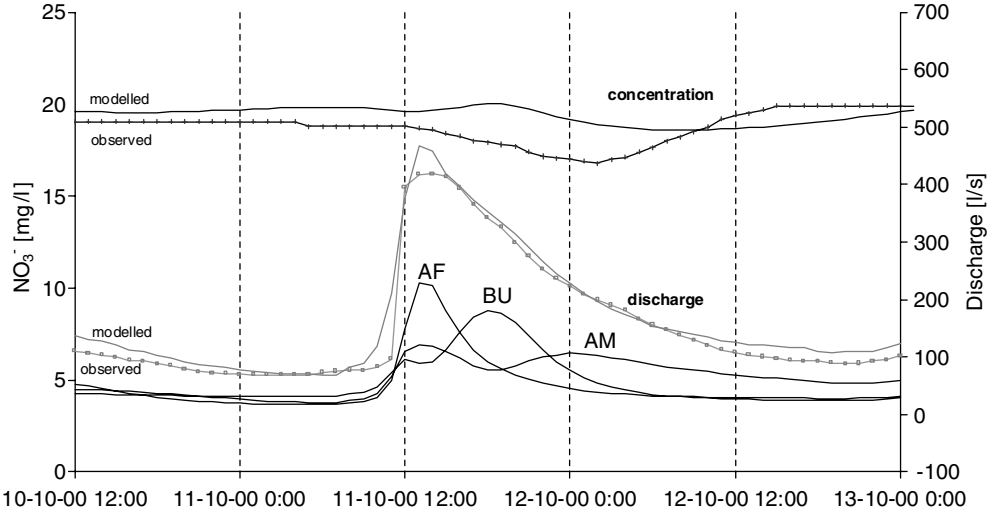

Figure 7 Simulation of the October 2000 flood event. The modelled curves (in plain) are compared with the observed curves (line with symbols). Chemographs are in black and hydrographs in gray. The curves labeled AM, AF, BU indicate the respective contribution of the AM, BU, AF tributaries to the spring discharge SAI throughout the flood.

water appearing simultaneously with the flood peak is attributed to a piston effect: at low stage preceding the flood, AM water is more abundant than water from AF and BU. This secondary peak also occurs for the January 2001 flood event.

January 2001 flood event

Peak flood discharge is slightly overestimated by the model, and the falling limb is delayed (Fig. 8). These differences could partly result from uncertainties in the AF's discharge rates, or from underestimation of the springs discharge rates (losses in the phreatic zone). The modelled chemograph closely matches the observed chemograph, although the negative peak is slightly accentuated.

Similar to the October 2000 simulation, the model shows the successive preferential contribution of waters from AF, BU, and AM and a lag between AF and BU peaks of only 2 h. Hydrograph recession is largely dominated by AM's water.

Conclusions

The fit between modelled and observed hydrographs and chemographs is satisfactory, especially when considering

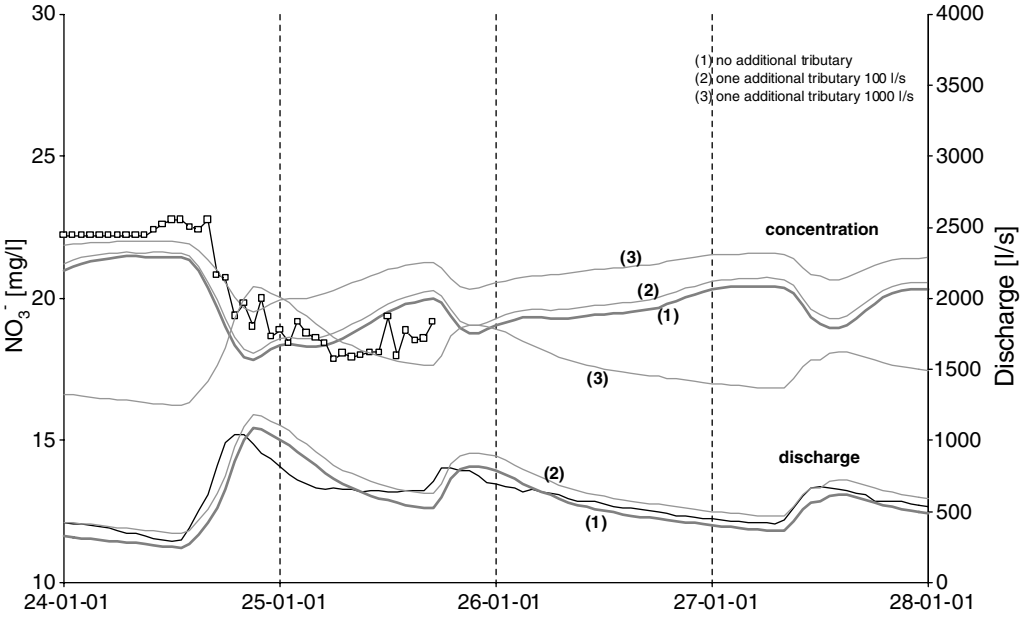

Figure 8 Simulation of the January 2001 flood event. Observed curves are in black and simulated curves in gray. Three simulations scenarios are presented. The first, curves (1), is the original tributary mixing model. The two other scenarios, curves (2) and (3), present the model sensitivity to an additional tributary. The input concentration of this additional tributary is 22.2 mg/l and the input discharge is 100 l/s for (2) and 1000 l/s for (3).

the simplicity of the flow and transport model, and the approximated flow and chemographs at BU and AF tributaries. From a qualitative perspective, the observations are well reproduced. However, two major differences appear. The simulated peak discharge is higher than the measured peak, and the changes in concentration are delayed in the simulation. This delay seems to be linked to an underestimation of the flow velocities, which have been calibrated for low to medium discharge rates only. The use of flat chemographs for AF and BU is also probably an important reason for these delays. A turbulent flow model could also allow for more realistic velocities, as well as for a better fit in lag times.

Specific conductance curves

Between 1992 and 1996, specific conductance was continuously recorded at the three main tributaries (AM, BU, AF) and at the spring (SAI). Except for AF, discharge rates were also measured. Therefore, these data allow for testing the tributary mixing numerical model with almost a complete set of observed boundary conditions, i.e. the only missing data for the February 1996 flood event is the discharge rate at AF. Like in the previous simulations, the AF discharge was set equal to the BU discharge. A characteristic result is given in Fig. 9: The modelled specific conductance is similar to the observed one. Specific conductance measurements

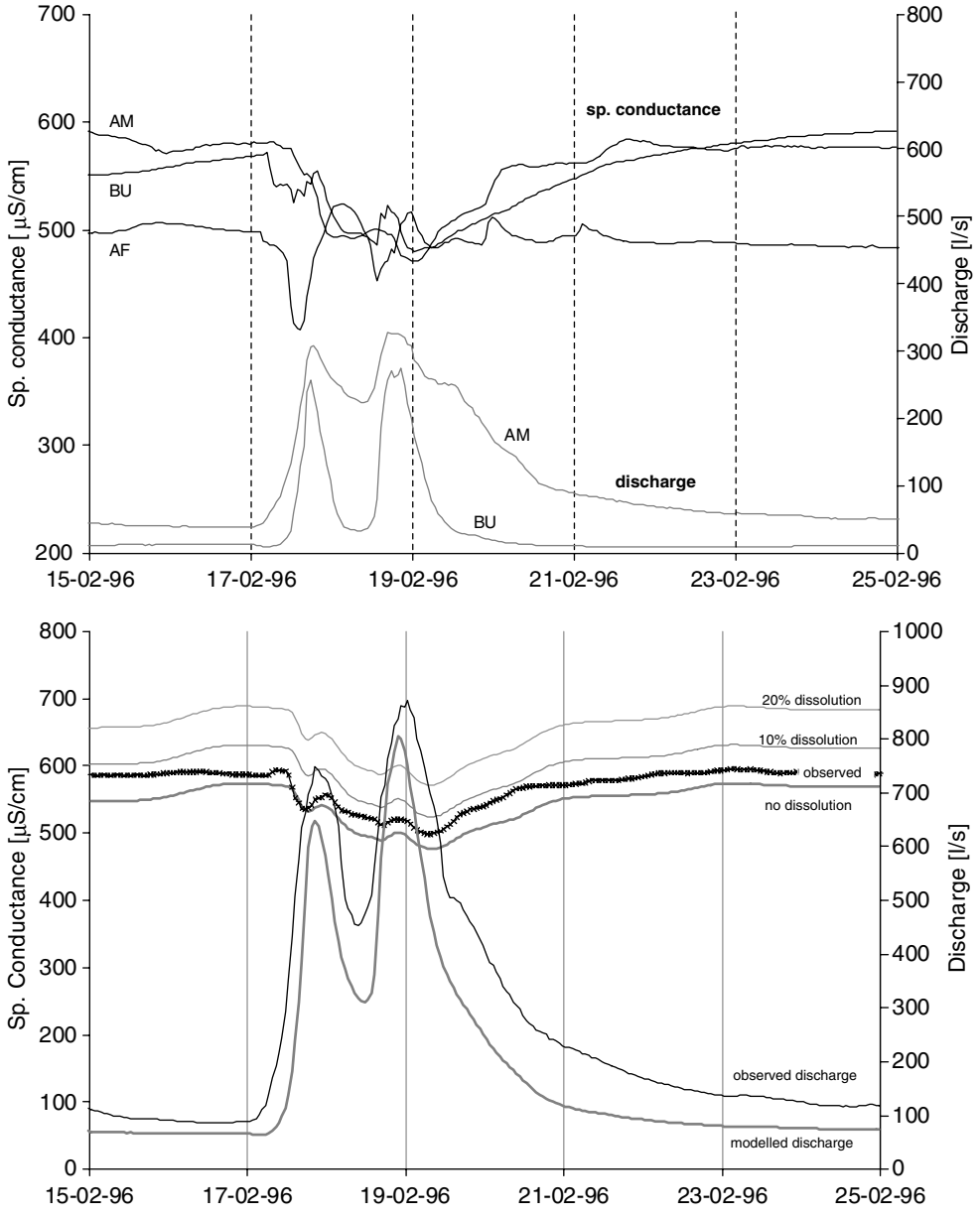

Figure 9 The upper graph presents the data used as boundary conditions for the simulation. The lower graph compares the results of the modelling with the observed specific conductance and discharge at the spring. The model sensitivity to dissolution is also represented.

were not accurately calibrated; this may explain the shift between the two curves. Modelled discharge is also close to the observed one.

Discussion

The following discussion is based on the above described results, and is also supported by observations of other flood events described in Perrin (2003).

The role of tributary mixing at the Milandre karst system

The modelling approach confirms qualitative interpretations made on chemographs during flood events. In the phreatic zone, tributary mixing is a major process that shapes the spring chemographs and hydrographs. A reasonable fit is obtained without having to consider (i) the dissolution in the conduits, (ii) the participation of any other mixing component (e.g. matrix storage). In order to test the sensitivity of the numerical model to (i) and (ii), two scenarios have been simulated:

- In the first, higher specific conductance values than those measured are assigned to the tributaries for the February 1996 flood event. This increase accounts for any conduit dissolution. Simulated outputs at the spring show that the fit remains acceptable if the specific conductance increase is not more than 10% (Fig. 9).
- In the second, an additional tributary accounts for a possible mixing component from matrix storage. Its boundary conditions do not vary and the assigned concentration corresponds to the measured concentration at the spring before the flood event (realistic assumption for matrix storage water chemistry). Simulations were carried out on the January 2001 flood event (Fig. 8). Simulated hydrographs and chemographs fit reasonably well if the contribution of matrix storage is less than 100 l/s (less than 10% of the total discharge). Chemographs are less sensitive than hydrographs because the matrix storage concentration is an average of all the input concentrations.

Hence the limited sensitivity of the model does not permit to conclude that conduit dissolution and/or matrix storage participation are not relevant during flood event. However these processes are not necessary for an acceptable simulation and if they are effective, their impact is limited (order of magnitude between 0 and 10%). Compared to conduit dissolution and matrix storage contribution, tributary mixing impacts strongly spring chemographs: if identical concentrations are used as tributary boundary conditions, the resulting chemographs differ to a large extent from the chemographs obtained with the observed tributary concentrations. The difference is particularly important when tributary concentrations are contrasted (i.e. in the case of spatially variable parameters such as nitrate or artificial tracers). Also Birk et al. (2004) showed no evidence for conduit dissolution in a gypsum karst aquifer during flood events. The limited/absent role of matrix storage is in agreement with Kiraly (1998) who showed that gradient inversion between conduits and low permeability volumes hinders water release from the low permeability volumes during floods. On the contrary, no water losses could be observed along the conduits. This shows that low permeability volume recharge during flood events is not significant. These observations pinpoint the limited role of matrix storage in the phreatic zone during flood events. This is consistent with what can be seen in the Milandre cave conduits: walls are made of compact limestone with a very low porosity. Also, dozens of tracer breakthrough curves have been observed along the Milandre cave conduits, and their analysis clearly showed that dispersion processes are not related to a water exchange with the low permeability volumes, but to variations of the flow cross-section and related eddies (Hauns et al., 2001). Hence in the authors' opinion, it is first necessary to consider the effect of tributary mixing before attempting any hydrograph separation by means of natural tracers.

It was also demonstrated that tributary mixing produces chemograph variations mainly if chemistries of the respective tributaries are contrasted (Fig. 6). This can provide information about the structure of the karst conduit network: Considering pollution-related parameters, which have a strong spatial variability (Perrin et al., 2003a), spring chemographs may look very different if the polluted tributaries are located downstream or upstream within the spring catchment area. On the contrary, dissolution-related parameters, which are usually more homogeneously distributed, produce more predictable chemographs at the spring (e.g. concentration decrease by dilution).

A conceptual model of flow and transport for the Milandre karst system

The results of this study need to be integrated into a conceptual model of the whole karst system. The data and interpretations related to the unsaturated zone are presented in Perrin et al. (2003b). At the Milandre system, recharge is diffuse and the respective sub-catchments have contrasting land-uses: mostly forests for the AF sub-catchment, meadows for the BU sub-catchment, and arable land for the AM sub-catchment (Fig. 10). Land-use controls groundwater chemistry to a large extent for pollution related parameters. Water is stored in reservoirs located in the upstream part of the sub-catchment (probably in the soil and the epikarst), and becomes saturated with respect to calcite. At low water stages, this ''perched'' groundwater is continuously released as base flow (Q_b) and feeds the tributaries. These base flows mix together (tributary mixing) in the phreatic zone to yield the spring water chemistry. Isotopic data from the unsaturated zone show two types of flood events (Perrin et al., 2003b): moderate flood events with no significant contribution of event water, and large flood events with event water participating to flood discharge. This differentiation is in agreement with observations in the phreatic zone:

In the case of a moderate flood event (e.g. October 2000 flood event), quick flow (Q_q), which is an overflow of the perched reservoirs, keeps the same chemical composition ($C_{1,2,3}$) as base flow. Chemical variations observed at the spring are moderate because they result from tributary mix-

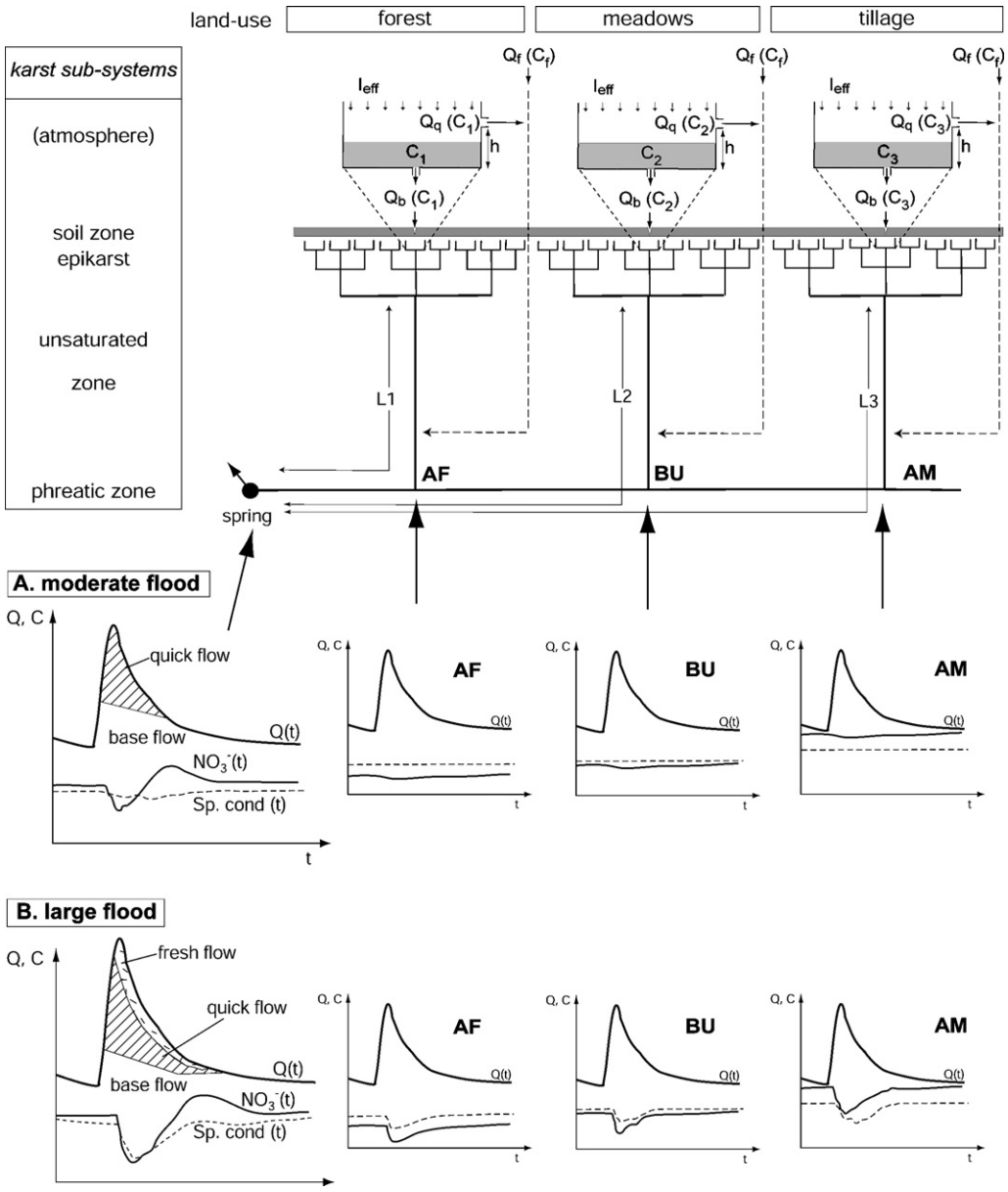

Figure 10 Conceptual model of flow and transport in the Milandre karst aquifer and resulting hydrographs and chemographs. At the top, a vertical cross-section through the aquifer is schematized with the respective locations of AF, BU, and AM tributaries; the hydraulic functioning of the epikarst is also represented. At the bottom, two different flood events are schematized: (a) a moderate flood event (no fresh flow), (b) large flood event. For each, the resulting hydrographs and chemographs are given for AM, BU, AF tributaries and the spring. For more details see text.

ing only: small changes occur in dissolution-related parameters since they have similar concentrations in the subcatchments. In contrast, pollution-related parameter chemographs vary more significantly at the spring since tributaries have contrasting concentrations. This case is illustrated by hydrograph A (Fig. 10).

In the case of a large flood event (e.g. January 2001 flood event), the actual recharge exceeds the soil and epikarst reservoir thresholds (h), and the remaining recharge water infiltrates directly into the system as fresh flow (Q_f) with the chemistry C_f. This water is undersaturated with respect to calcite and dilutes the base flow and quick flow components. Hence, both dissolution-related parameters and pollution-related parameters significantly vary at the spring (hydrograph B, Fig. 10).

This overall behaviour is illustrated by the two successive flood events of October 2001 (Fig. 11). The first flood is characterised by significant variations (nearly 8% of the pre-flood value) for the pollution related parameter (nitrate) and only slight changes (nearly 3% of the pre-flood value) for the dissolution related parameter (specific conductance). Hence, this flood event consists of base flow and quick flow only. The second flood, with higher discharge rates, presents an important dilution for both parameters (respectively 10% and 25% of the pre-flood values). The decrease in specific conductance is caused by tributary mixing

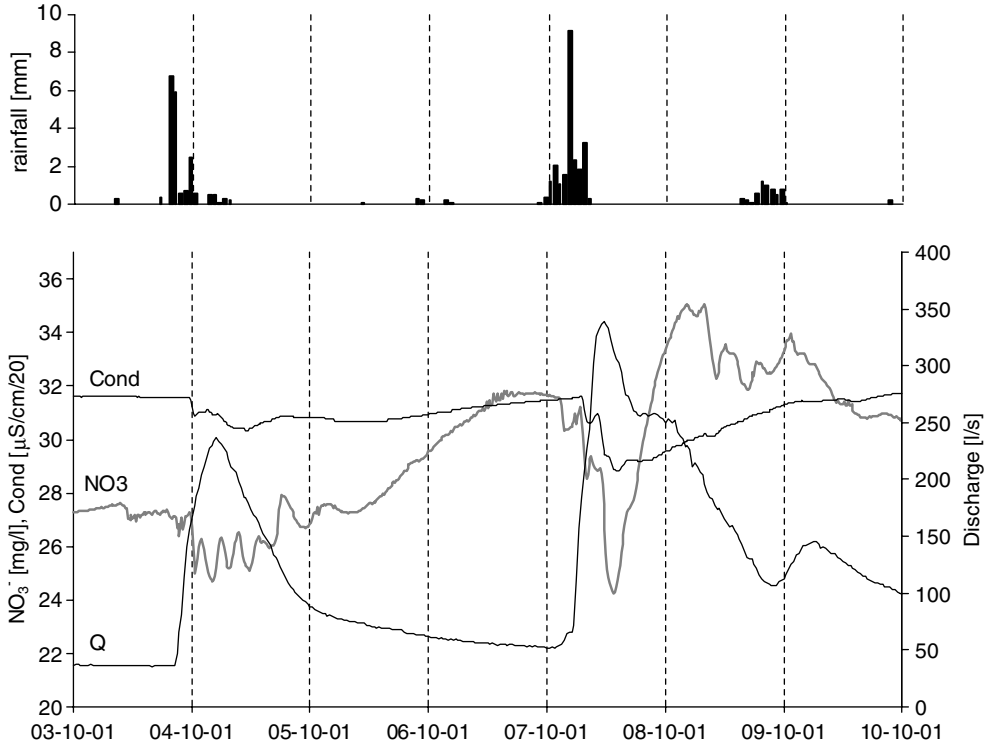

Figure 11 Evolution of specific conductance and nitrates concentration at Milandrine upstream (AM), in October 2001. Note that specific conductance values are divided by 20.

and by the mixing with fresh flow, which also accentuates the decrease in nitrate concentrations.

This aquifer behaviour has two important consequences:

(i) Moderate flood events could be used to detect the existence of tributaries with contrasting chemistry. Moreover it should be possible to infer their respective location with respect to the spring. However in practice, it may be difficult to find karst aquifers with well defined sub-catchments having their own specific groundwater chemistry.

(ii) Spring water vulnerability to accidental pollution increases suddenly during large flood events, when fresh flow by-passes the soil/epikarst reservoirs and reaches the spring within hours or a few days. In contrast, mean residence times of base flow and quick flow are on the order of weeks or months.

Extension of the model to other karst systems

Generally speaking, one can define three main types of karstic aquifers discharging at springs (for more details see Perrin (2003) who summarized the available literature): deep phreatic karst systems with autogenic recharge (type 1), shallow karst systems with autogenic recharge (type 2), and allogenic karst systems with allogenic and autogenic recharge (type 3). The Milandre karst system is typically a shallow karst. In allogenic karst systems, spring chemographs are strongly influenced by the contribution of allogenic streams during flood events (Vervier, 1990; Groves, 1992; Wicks and Engeln, 1997). In such a case, the conceptual model proposed in the present paper is not adequate. The major difference between types 1 and 2 is the size (mainly thickness) of the phreatic zone. The large extent of the phreatic zone for type 1 karst systems may have significant consequences on transport (Vaute et al., 1997; Motyka, 1998; Martin and Dean, 2001). The role of low permeability volumes will be more important in the case of aquifers having higher matrix hydraulic conductivity and effective porosity such as the simulated scenarios shown by Birk et al. (2005, 2006).

Hence, our observations and conclusions apply mainly to shallow karst systems (type 2). However it is clear that tributary mixing also exists in the two other types of karst systems, and has to be taken into account, although its significance is not clear at this stage. In the Milandre karst, the tributary mixing approach is straightforward because the main tributaries are accessible and have been measured. This type of observation has been carried out only in a very restricted number of systems. This is probably the main reason why this process was not considered for data interpretations in most of the existing studies.

Conclusions

It could appear trivial to say that springs hydrographs and chemographs result from the mixing of the system's main tributaries (i.e. a result of tributary mixing). But to the authors' knowledge, the effect of tributary mixing was only qualitatively described by Hess and White (1988) so far. The absence of publications on the tributary mixing process is probably due to the fact that most studies used data from springs only. The proposed tributary mixing model, which considers only the relative contribution of the Milandre

system three main tributaries, can reproduce karst spring chemographs and hydrographs. This leads to two important conclusions concerning transport of chemicals in the phreatic zone:

(i) transport is mainly non-reactive, even during flood events;
(ii) no significant mixing component with water stored in the low permeability volumes occurs in the phreatic zone.

These observations apply at least to shallow karst systems in compact limestone, comparable to the Milandre site. Chemical reactions (e.g. limestone dissolution) mainly occur in the unsaturated part of the system, most probably in the soil and epikarst zones. It means that the chemistry of the tributaries is determined in the upstream part of the system. Hence dissolution models (e.g. Shuster and White, 1971; Ternan, 1972; Grasso and Jeannin, 2002; Grasso et al., 2003) or mixing models with a matrix storage component (e.g. Blavoux and Mudry, 1983; Dreiss, 1989; Vervier, 1990; Lee and Krothe, 2001; Maloszewski et al., 2002) are not directly applicable to the studied karst aquifer. It appears necessary to first assess the role of tributary mixing before attempting any hydrograph separation technique or estimating any dissolution process.

Springs chemographs show two types of response: (1) In the case of moderate flood events, concentrations of pollution-related parameters vary more significantly at the spring than dissolution-related parameters. (2) During large flood events, pollution-related and dissolution-related parameters present significant concentration variations at the spring. The general trend results in a concentration decrease of dissolution-related parameters due to the mixing with fresh infiltrated water.

Two practical consequences result from this behaviour: (1) the existence of tributaries could be theoretically inferred from the analysis of spring chemographs; (2) the vulnerability of karst springs with respect to accidental pollution suddenly increases during large flood events, when fresh infiltrated water reaches the spring within hours or a few days (i.e. transit times are strongly shortened). The applicability of (1) is probably limited since the natural tracers' concentration contrasts between the various tributaries are generally small. However, some further developments may be obtained by the adequate use of artificial tracers which by definition will present high contrasts.

The presented approach should be included into a more comprehensive groundwater model of karst aquifers, also integrating the low permeability volumes. This will lead to a qualitative evaluation of the effect of matrix storage, especially in deep phreatic karst systems. Moreover, observations similar to those obtained at Milandre test site should be made at other systems in order to test the applicability of tributary mixing. It must be pointed out that tributary mixing is implicitly implemented into deterministic numerical models that can handle discrete conduits and fissures. Our data and simulations show that the branching of the conduit network strongly influences the response at the spring. Therefore, distributed models are required to further study and interpret karst spring chemographs.

Acknowledgements

This project was supported by the Swiss National Science Foundation, Grant no. 20-61717.00. We are indebted to the Jura Caving Club for access to the cave. At the Centre of Hydrogeology, T. Ettlin, F. Bourret, B. Wenger and S. Cattin gave us priceless support for the field and the lab work. We thank the editor and the two anonymous reviewers for their fruitful comments.

References

Benderitter, Y., Roy, B., Tabbagh, A., 1993. Flow characterization through heat transfer evidence in a carbonate fractured medium: first approach. Water Resources Research 29 (11), 3741—3747.

Birk, S., Sauter, M., Liedl, R., 2001. Process-based modelling of concentration and temperature variations at a karst spring. In: Proc. 7th Conf. on Limestone Hydrology and Fissured Media, Besancon, pp. 41—44.

Birk, S., Liedl, R., Sauter, M., 2002. Characterisation of gypsum karst aquifers by heat and solute transport simulations. Acta Geol. Polon. 52 (1), 23—29.

Birk, S., Liedl, R., Sauter, M., 2004. Identification of localised recharge and conduit flow by combined analysis of hydraulic and physico-chemical spring responses (Urenbrunnen, SW-Germany). Journal of Hydrology 286, 179—193.

Birk, S., Geyer, T., Liedl, R., Sauter, M., 2005. Process-based interpretation of tracer tests in carbonate aquifers. Ground Water 43 (3), 381—388.

Birk, S., Liedl, R., Sauter, M., 2006. Karst spring responses examined by process-based modeling. Ground Water, Online first.

Blavoux, B., Mudry, J., 1983. Décomposition chimique des hydrogrammes du karst. Hydrogéologie-Géologie de l'Ingénieur 4, 270—278.

Cornaton, F., 2004. Deterministic models of groundwater age, life expectancy and transit time distributions in advective-dispersive systems. Neuchâtel, Neuchâtel. Available from: <www.unine.ch/biblio/bc/theses_pdf/these_CornatonF.pdf>.

Cornaton, F., Perrochet, P., 2002. Analytical 1 D dual-porosity equivalent solutions to 3D discrete single-continuum models. Application to karstic spring hydrograph modelling. Journal of Hydrology 262, 165—176.

Dreiss, S.J., 1989. Regional scale transport in a karst aquifer: 1. Component separation of spring flow hydrographs. Water Resources Research 25 (1), 117—125.

Grasso, D-A., Jeannin, P-Y., 1994. Estimation des pertes dans la partie aval du réseau karstique de la Milandrine: bilan hydrique au sein d'un aquifère karstique. Bulletin d'Hydrogéologie 13, 115—128.

Grasso, D.A., Jeannin, P-Y., 2002. A global experimental approach of karst springs hydrographs and chemographs. Groundwater 40 (6), 608—618.

Grasso, D.A., Jeannin, P-Y., Zwahlen, F., 2003. A deterministic approach to the coupled analysis of karst spring hydrographs and chemographs. Journal of Hydrology 271, 65—76.

Gretillat, P.-A., 1996. Les aquifères karstiques et poreux de l'Ajoie (Jura, Suisse), Neuchâtel, Neuchâtel, 209 pp.

Groves, C.G., 1992. Geochemical and kinetic evolution of a karst flow system: Laurel creek, West Virginia. Groundwater 30 (2), 186—191.

Hauns, M., Jeannin, P-Y., Atteia, O., 2001. Dispersion, retardation and scale effect in tracer breakthrough curves in karst conduits. Journal of Hydrology 241, 177—193.

Hess, J.W., White, W.B., 1988. Storm response of the karstic carbonate aquifer of south-central Kentucky. Journal of Hydrology 99, 235—252.

Jeannin, P-Y., 2001. Modeling flow in phreatic and epiphreatic karst conduits in the Hölloch cave (Muotatal, Switzerland). Water Resources Research 37 (2), 191—200.

Jeannin, P.-Y., 1998. Structure et comportement hydraulique des aquifères karstiques, Neuchâtel, Neuchâtel, 237 pp.

Jeannin, P.-Y., Grasso, D.A., 1995. Estimation des infiltrations efficaces journalières sur le bassin karstique de la Milandrine. Bulletin d'Hydrogéologie 14, 83—94.

Jeannin, P.-Y., Maréchal, J.-C., 1995. Lois de pertes de charge dans les conduits karstiques: Base théorique et observations. Bulletin d'Hydrogéologie 14, 149—176.

Kiraly, L., Mueller, I., 1979. Hétérogénéité de la perméabilité et de l'alimentation dans le karst: effet sur la variation du chimisme des sources karstiques. Bulletin du Centre d'Hydrogéologie 3, 237—285.

Kiraly, L., 1998. Modelling karst aquifers by the combined discrete channel and continuum approach. Bulletin d'Hydrogéologie 16, 77—98.

Lakey, B., Krothe, N.C., 1996. Stable isotopic variation of storm discharge from a perennial karst spring, Indiana. Water Resources Research 32 (3), 721—731.

Lee, E.S., Krothe, N.C., 2001. A four-component mixing model for water in a karst terrain in south-central Indiana; USA. Using solute concentration and stable isotopes as tracers. Chemical Geology 179, 129—143.

Maloszewski, P., Stichler, W., Zuber, A., Rank, D., 2002. Identifying the flow systems in a karstic-fissured-porous aquifer, Schneealpe, Austria, by modelling of environmental 18O and 3H isotopes. Journal of Hydrology 256, 48—59.

Mangin, A., 1975. Contribution à l'étude hydrodynamique des aquifères karstiques. Annales de spéléologie (29/3), 283—332, 29/4: 495—601, 30/1: 21—124.

Maréchal, J-C., 1994. Etude et modélisation de l'hydraulique et du transport dans les drains karstiques. MSc. Thesis Hydrogeology Centre, Neuchâtel University. 128 pp.

Martin, J.B., Dean, R.W., 2001. Exchange of water between conduits and matrix in the Floridan aquifer. Chemical Geology 179, 145—165.

Motyka, J., 1998. A conceptual model of hydraulics networks in carbonate rocks illustrated by examples from Poland. Hydrogeology Journal 6 (4), 469—482.

Palmer, A., 1991. The origin and morphology of limestone caves. Geol. Soc. of America Bull. 103, 1—21.

Perrin, J., 2003. A conceptual model of flow and transport in a karst aquifer based on spatial and temporal variations of natural tracers. Neuchâtel, Neuchâtel, 188 pp. Available from: <www.unine.ch/biblio/bc/theses_pdf/these_PerrinJ.pdf>.

Perrin, J., Wenger, B., 2001. Continuous measurement of nitrates concentrations, lab tests and field results in a karstic aquifer. In: Mudry, J., Zwahlen, F. (Eds.), 7th Conference on Limestone hydrology and Fissured media. Univ. de Besançon, pp. 277—280.

Perrin, J., Jeannin, P.-Y., Zwahlen, F., 2003a. Implications of the spatial variability of the infiltration water chemistry for the investigation of a karst aquifer. Hydrogeology Journal 11, 673—686.

Perrin, J., Jeannin, P.-Y., Zwahlen, F., 2003b. Epikarst storage in a karst aquifer: a conceptual model based on isotopic data. Milandre test site, Switzerland. Journal of Hydrology 279, 106—124.

Plagnes, V., Bakalowicz, M., 2001. May it propose a unique interpretation for karstic spring chemographs? In: Mudry, J., Zwahlen, F. (Eds.), 7th Conference on Limestone Hydrology and Fissured Media. Franche-Comté University, Besançon, pp. 293—298.

Sauter, M., 1992. Quantification and forecasting of regional groundwater flow and transport in a karst aquifer (Gallusquelle, SW Germany), Tübingen, Tübingen, 151 pp.

Shuster, E.T., White, W.B., 1971. Seasonal fluctuations in the chemistry of limestone springs: A possible means for characterizing carbonate aquifers. Journal of Hydrology 14, 93—128.

Ternan, J.L., 1972. Comments on the use of a calcium hardness variability index in the study of carbonate aquifers; with references to the central Pennines, England. Journal of Hydrology 16, 317—321.

Vaute, L., Drogue, C., Garrelly, L., Ghelfenstein, M., 1997. Relations between the structure of storage and the transport of chemical compounds in karstic aquifers. Journal of Hydrology 199, 221—238.

Vervier, P., 1990. Hydrochemical characterization of the water dynamics of a karstic system. Journal of Hydrology 121, 103—117.

White, W.B., 1988. Geomorphology and Hydrology of Karst Terrains. Oxford University Press, Oxford, 464 pp.

Wicks, C.M., Engeln, J.F., 1997. Geochemical evolution of a karst stream in Devils Icebox Cave, Missouri, USA. Journal of Hydrology 198, 30—41.

Williams, P.W., 1983. The role of the subcutaneous zone in karst hydrology. Journal of Hydrology 61, 45—67.